

## Article

# Nanoparticles and Plant By-Products for Edible Coatings Production: A Case Study with Zinc, Titanium, and Silver

Alexandra Tauferová , Zdeňka Javůrková , Matej Pospiech, Hana Koudelková Mikulášková, Karolína Těšíková, Dani Dordevic , Simona Dordevic  and Bohuslava Tremlová \* 

Department of Plant Origin Food Sciences, Faculty of Veterinary Hygiene and Ecology, University of Veterinary Sciences Brno, Palackého tř. 1946/1, 612 42 Brno, Czech Republic; tauferovaa@vfu.cz (A.T.); javurkovaz@vfu.cz (Z.J.); pospiechm@vfu.cz (M.P.); koudelkovamih@vfu.cz (H.K.M.); tesikovak@vfu.cz (K.T.); dordevicd@vfu.cz (D.D.); dordevics@vfu.cz (S.D.)

\* Correspondence: tremlovab@vfu.cz

**Abstract:** For the development of functional edible packaging that will not lead to rejection by the consumer, it is needed to analyze the interactions between ingredients in the packaging matrix. The aim of this study was to develop edible chitosan-based coatings that have been enriched with red grape extracts, zinc, silver, and titanium nanoparticles. The organoleptic properties of the produced edible packaging were described by quantitative descriptive analysis and consumer acceptability was verified by hedonic analysis. By image analysis, color parameters in the CIELab system, opacity, Whiteness and Yellowness Index were described. The microstructure was described by scanning electron microscopy. The hedonic evaluation revealed that the addition of nanometals and their increasing concentration caused a deterioration in sample acceptability. The overall evaluation was higher than 5 in 50% of the samples containing nanometals. The addition of nanometals also caused statistically significant changes in  $L^*$ ,  $a^*$ , and  $b^*$  values. The sample transparency generally decreased with the increasing concentration of nanoparticle addition. Scanning electron microscopy showed, that the addition of nanometals does not disrupt the protective function of the packaging. From a sensory point of view, the addition of ZnO nanoparticles in concentrations of 0.05 and 0.2% appeared to be the most favorable of all nanometals.

**Keywords:** packaging; nanoparticles; sensory properties; scanning electron microscopy; CIELab; plant extract



**Citation:** Tauferová, A.; Javůrková, Z.; Pospiech, M.; Koudelková Mikulášková, H.; Těšíková, K.; Dordevic, D.; Dordevic, S.; Tremlová, B. Nanoparticles and Plant By-Products for Edible Coatings Production: A Case Study with Zinc, Titanium, and Silver. *Polymers* **2022**, *14*, 2837. <https://doi.org/10.3390/polym14142837>

Academic Editor: Carola Esposito Corcione

Received: 30 May 2022

Accepted: 9 July 2022

Published: 12 July 2022

**Publisher's Note:** MDPI stays neutral with regard to jurisdictional claims in published maps and institutional affiliations.



**Copyright:** © 2022 by the authors. Licensee MDPI, Basel, Switzerland. This article is an open access article distributed under the terms and conditions of the Creative Commons Attribution (CC BY) license (<https://creativecommons.org/licenses/by/4.0/>).

## 1. Introduction

With the increasing demands on packaging technologies, the development of new types of packaging materials is becoming more important. This development raises a number of issues related to environmental pollution and waste recycling [1].

Therefore, attention is currently being paid to research into biodegradable packaging materials made from renewable raw materials that are environmentally friendly. Edible packaging seems to be a suitable alternative to plastic materials and represents great potential in a number of different areas [2].

An important factor in the development of edible packaging is the combination of knowledge of biodegradable materials and the food packaging sector. Based on the results of a number of studies, it is possible to state a significant effect of edible packaging on maintaining quality and prolonging shelf life, for example in fresh or sliced food [3]. Studies also point to the functionality of edible packaging as an effective barrier on the surface of food, which has the ability to reduce water loss or modify the internal atmosphere, which can slow down some of the processes that lead to their aging [4]. Another potential benefit of edible packaging is their use as carriers of active ingredients that increase antioxidant capacity or improve antibacterial properties that limit the growth of pathogens on the food surface [5,6].

Current research in the food sector has been significantly influenced by nanotechnology which also involves the development of functional edible food packaging. The use of nanoparticles in the production of edible packaging seems to be very promising. Individual studies deal with the use of artificial nanoparticles, which are added to food packaging as a functional component. Their indisputable advantage is increasing food stability, reducing the growth of bacteria, fungi, and yeasts, or, in some cases, protecting light-sensitive foods [6,7]. The incorporation of nanoparticles into edible materials has contributed to the development of novel edible materials called nanocomposites. Silver, zinc oxide, and titanium dioxide are among the most used inorganic nanoparticles [8]. Considering specifically the improved food packaging physical properties, the incorporation of silver nanoparticles may contribute to the increased oxygen and water vapor barrier properties, and the addition of zinc oxide nanoparticles may lead to improved mechanical and heat seal properties, both with reduced oxygen permeability. Moreover, zinc oxide nanoparticles have the potential to mask the intense aroma of antimicrobial essential oils and improve their activity. Photoinduced titanium oxide nanoparticles act as oxygen and ethylene scavengers [9]. Of course, the concentration of selected nanoparticles affects both the individual physical properties of the edible packaging and plays a vital role to achieve an adequate antimicrobial effect [10].

In addition to the functional and mechanical properties of edible packaging, an essential and often monitored parameter is their color and transparency, in particular, because of the overall appearance of the packaging which entails positive consumer reactions [11]. Consumer preferences are one of the basic factors determining the usability of new products and this also applies to the sensory properties of edible packaging, which significantly affect the acceptance of final products [12].

Although various additives may improve the functional or nutritional properties of edible packaging, they may also lead to a deterioration in the mechanical or sensory properties and, consequently, to rejection by the consumer. For the development of functional edible packaging with high sensory performance, further studies are needed to shed more light on the interactions between individual functional ingredients in the edible packaging matrix [13].

This study builds on previous studies confirming the suitability of adding red grape extract to chitosan-based edible packaging in terms of its superior antimicrobial properties and antioxidant capacity compared to other alternatives to the investigated plant by-products. [14]. The concentration of 10% was selected with regard to sensory acceptability, as a higher concentration of grape extract resulted in a more intense color of the packaging and thus lower sensory acceptability [15].

In view of the above, the aim of this study was to develop edible chitosan-based coatings that have been enriched with zinc, silver, and titanium nanoparticles. Red grape extracts have also been used as a suitable source of bioactive ingredients.

## 2. Materials and Methods

### 2.1. Packaging Preparation

#### 2.1.1. Production of Packaging with the Addition of Nanoparticles

ZnO and TiO<sub>2</sub> nanoparticles were weighed for packaging preparation in concentrations of 0.05, 0.2, and 0.5%. Subsequently, 135.0 mL of 1.0% lactic acid dissolved in distilled water was added with the addition of 1.5 g of chitosan. The mixture was then heated and stirred on a magnetic stirrer for 15 min at 50 °C at 750 rpm, and afterward, 0.75 mL of glycerol was added and stirred again for 5 min. The prepared film-forming solution was poured into a 15.0 cm diameter Petri dish, where it was allowed to dry for 48 h. The preparation procedure was similar for samples containing the red grape extract. After stirring for 15 min, 13.5 mL of the extract was added, and at the same time, 13.5 mL less lactic acid was initially used.

### 2.1.2. Production of Packaging with the Addition of Colloidal Silver

To prepare edible packaging with the addition of colloidal silver, 1.5 g of chitosan was weighed and 135.0 mL of 1% lactic acid dissolved in colloidal silver at concentrations of 10, 30, and 50 ppm was added (Table 1). The mixture was stirred and then heated on a magnetic stirrer for 15 min at 50 °C and 750 rpm. Subsequently, 0.75 mL of glycerol was added, stirred for 5 min, and poured into 15.0 cm diameter Petri dishes, where they were allowed to dry for 48 h. The thickness of the experimentally produced edible packaging was  $0.21 \pm 0.01$  mm.

**Table 1.** Composition of the coatings produced.

Sample	Composition
Ctrl	Chitosan + 1% lactic acid + glycerol
CtrlGR	Chitosan + 1% lactic acid + 10% extract * + glycerol
Zn_005	Chitosan + 1% lactic acid + 0.05% nano ZnO + glycerol
Zn_02	Chitosan + 1% lactic acid + 0.2% nano ZnO + glycerol
Zn_05	Chitosan + 1% lactic acid + 0.5% nano ZnO + glycerol
Ti_005	Chitosan + 1% lactic acid + 0.05% nano TiO <sub>2</sub> + glycerol
Ti_02	Chitosan + 1% lactic acid + 0.2% nano TiO <sub>2</sub> + glycerol
Ti_05	Chitosan + 1% lactic acid + 0.5% nano TiO <sub>2</sub> + glycerol
Ag_10	Chitosan + 1% lactic acid + colloidal Ag 10 ppm + glycerol
Ag_30	Chitosan + 1% lactic acid + colloidal Ag 30 ppm + glycerol
Ag_50	Chitosan + 1% lactic acid + colloidal Ag 50 ppm + glycerol
ZnGR_005	Chitosan + 1% lactic acid + 0.05% nano ZnO + 10% extract * + glycerol
ZnGR_02	Chitosan + 1% lactic acid + 0.2% nano ZnO + 10% extract * + glycerol
ZnGR_05	Chitosan + 1% lactic acid + 0.5% nano ZnO + 10% extract * + glycerol
TiGR_005	Chitosan + 1% lactic acid + 0.05% nano TiO <sub>2</sub> + 10% extract * + glycerol
TiGR_02	Chitosan + 1% lactic acid + 0.2% nano TiO <sub>2</sub> + 10% extract * + glycerol
TiGR_05	Chitosan + 1% lactic acid + 0.5% nano TiO <sub>2</sub> + 10% extract * + glycerol
AgGR_10	Chitosan + 1% lactic acid + colloidal Ag 10 ppm + 10% extract * + glycerol
AgGR_30	Chitosan + 1% lactic acid + colloidal Ag 30 ppm + 10% extract * + glycerol
AgGR_50	Chitosan + 1% lactic acid + colloidal Ag 50 ppm + 10% extract * + glycerol

\* Red grape extract.

### 2.1.3. Grape Marc Preparation

Red grapes of Scarlotta Seedless variety grown in South Africa and purchased in the regular market network (Tesco, Brno, Czech Republic) were used for the production of marc. The juice was obtained from the red grapes using a Catler JE 4011 juicer. The by-product of the juice production, the marc, was then transferred to bags and frozen for further use.

### 2.1.4. Extract Preparation

From the thawed marc, 10.0 g was weighed to which 100.0 mL of boiling distilled water (100 °C) was added, and 10 min later filtration was performed (Whatmann KA-1 filter paper), the extract at room temperature was then used to prepare the packaging.

## 2.2. Sensory Analysis

The key organoleptic properties of edible packaging were described by quantitative descriptive analysis and consumer acceptability was verified by hedonic analysis. As the actual use of edible packaging in practice to date is only small, a questionnaire survey was conducted among the evaluators in order to research deeper their perception of the use of produced edible packaging for selected food groups.

### 2.2.1. Quantitative Descriptive Analysis

Quantitative descriptive analysis and hedonic analysis were performed at the Institute of Plant Hygiene and Food Technology, FVHE, VETUNI. A panel of 14 trained evaluators, who had previous experience in evaluating edible packaging, participated in the

quantitative descriptive analysis. For the purpose of quantification of attributes, 9-degree categorical ordinal scales with described extremes from 1 (minimum intensity) to 9 (highest intensity) were used. The evaluated descriptors included color intensity, odor intensity, surface character, flexibility, stickiness, and overall rating. Quantitative descriptive analysis was performed twice.

### 2.2.2. Hedonic Analysis

Based on the results of the analysis performed by the trained panel, 11 samples were selected from a total of 20 samples, which achieved an average score higher than 5 in the overall evaluation. These 11 selected samples were subsequently evaluated by hedonic analysis, in which 65 untrained evaluators from among students and employees of the University of Veterinary Sciences Brno participated. Descriptors including pleasantness of appearance, pleasantness of aroma, pleasantness of texture, and overall evaluation were measured using a 9-digit category ordinal hedonic scale, where 1 meant an extremely unpleasant sensation, 5 meant a neutral sensation, and 9 the highest degree of pleasantness.

### 2.2.3. Assessment of the Probability of Purchasing Food Commodities in Edible Packaging

The hedonic evaluation also assessed the probability of purchasing products, such as fruit, vegetables, meat products, bakery products, and milk products (cheese), in individual samples of edible packaging. For the purposes of this evaluation, a 5-point scale was used, where 1 meant the lowest willingness to consume the product in the given edible packaging, 3 meant a neutral attitude, and 5 meant that the evaluator would certainly be willing to consume the given commodity in the given packaging.

### 2.3. Evaluation of Color and Color Properties of Packaging

The samples were placed in 150.0 mm Petri dishes. Digital images of all samples were obtained by a computer vision system. Scanning was performed under standard lighting conditions, which were provided by Osram Delux L—1 × 18 W lamps (OSRAM GmbH., Munich, Germany) and scanning in a dark chamber. Individual images were taken by a Canon EOS 600D camera (Canon, Tokyo, Japan) mounted on a tripod (Fomei CS 920, Hradec Králové, Czech Republic) against a white and a black background. The shooting mode was in manual setting: exposure time 1/15, aperture F 8.0, image size L, sensitivity ISO 100 [16]. Each sample was captured 10 times.

Subsequently, the images were processed by Nikon Imaging Software NIS-Elements BR 4.13.04 (Laboratory Imaging s.r.o., Prague, CZE). The same area of the circle (ROI—region of interest) was always selected for evaluation within NIS-Elements. Subsequently, the color characteristics of MeanRed, MeanGreen, and MeanBlue were measured and then converted to CIEL\*a\*b\* system where  $L^*$  means lightness,  $a^*$  indicates the position on the red–green axis, and  $b^*$  on the yellow–blue axis.

The difference between samples and control ( $\Delta E$ ) was also monitored. This parameter was calculated using the equation of CIE  $\Delta E_{2000}$  [17,18].

#### 2.3.1. Opacity

Another monitored parameter was the opacity of the packaging. This was obtained by calculation according to the following Equation (1):

$$\% \text{ Opacity} = \frac{(L^* \text{ black})}{(L^* \text{ white})} * 100 \quad (1)$$

where  $L^*$  black was obtained from the measurement values of images taken on a black background and  $L^*$  white on a white background. A value of 100% indicates opaque packaging and a value of 0% indicates transparent packaging [19].



### 2.3.2. Whiteness Index

Another parameter was the Whiteness Index, which was obtained by Equation (2) given in Li et al., 2019 [20]:

$$\text{Whiteness Index} = 100 - \sqrt{(100 - L^*)^2 + a^{*2} + b^{*2}} \quad (2)$$

where  $L^*$  is the value obtained from the measurement calculations on the white background,  $a^*$  indicates the position on the red–green axis, and  $b^*$  on the yellow–blue axis.

### 2.3.3. Yellowness Index

In their work, Saberi et al. (2016) used the parameter of the Yellowness Index for the evaluation. This parameter is obtained by the following, Equation (3) [21]:

$$\text{Yellowness Index} = \frac{142.86 b^*}{L^*} \quad (3)$$

where  $L^*$  is the value obtained from the measurement calculations on the white background and  $b^*$  indicates the position on the yellow–blue axis.

## 2.4. Evaluation of the Surface of Edible Packaging by SEM

The microstructure of experimentally produced edible packaging was described by SEM, primarily the particle distribution, crystal formation, degree of phase segregation, and the formation of cracks related to the barrier properties of the packaging.

The surface and fracture of the edible packaging were evaluated. The surface evaluation of the edible packaging was performed after forming the gel on a conductive target so as to minimize surface changes caused by bending or fracturing during handling.

For fracture analysis, the edible film formed in the standard way (in compliance with Sections 2.1.1 and 2.1.2) was frozen with liquid nitrogen and subsequently mechanically broken. The fragments were applied to a carbon double-sided adhesive tape. The samples were gilded with 10 nm on a Q150R ES sample plating device (Quorum Technologies, Laughton, UK) and subsequently examined in triplicate with a MIRA3 TESCAN microscope (Tescan, a.s., Brno, Czechoslovakia), at a voltage of 5.0 kV. Magnification 1kx, 10kx and refraction, 3kx surface images. The exact magnification is shown on the individual micrographs.

Total area and nearest fissure distance were measured on microphotographs by the imaging analysis software NIS Element (Laboratory Imagine, Prague, Czechoslovakia). The nearest object's distance was calculated as the smallest distance to another object (measured between their centers of gravity). The area was calculated by the following, Equation (4):

$$\text{Area} = \sum \text{pixel} \quad (4)$$

## 2.5. Statistical Analysis

The results of the sensory analysis of the coatings were evaluated by the R statistical software (The R Foundation for Statistical Computing, Vienna, Austria) using the SensoMineR package. Sensory data were processed by the principal component analysis (PCA) method.

Color parameters were statistically evaluated using the Unistat Tukey-HSD test procedure (Unistat Ltd., London, UK). The K samples test (Kruskal–Wallis test with Dunn multiple comparisons) by statistical software XLSTAT 2021 (Addinsoft, Paris, FR) was used for statistical comparison of the total area and nearest fissure distance.

## 3. Results and Discussion

### 3.1. Results of Sensory Analysis of Edible Packaging

#### 3.1.1. Quantitative Descriptive Analysis

Factor analysis (Figure 1a) confirmed a close correlation between color intensity and odor intensity. Conversely, a negative correlation was confirmed between the descriptors of

surface roughness (values ranging from the lowest for a smooth surface to the highest for a rough surface) and stickiness. The principal component analysis results graph explains 83.22% variability using the two principal components, with the first component explaining 50.00% and the second component 33.22% variability. From the sample map (Figure 1b) and from Table 2 showing statistically significant ( $p < 0.05$ ) differences between individual edible films, it can be seen that there were a number of statistically significant differences between individual edible packaging samples. The remote sample Zn\_05, characterized by high surface roughness and at the same time very low values of color intensity, odor intensity, stickiness, and flexibility, was clearly singled out on the sample map. The second remote sample was the ZnGR\_05 sample, which was also characterized by high surface roughness, low stickiness, and flexibility, but at the same time statistically significantly higher odor and color intensity. Samples containing grape extract generally belonged to samples characterized by more intense color and aroma, due to the presence of typical anthocyanin pigments and a number of characteristic volatile aromatic substances [22,23]. The control sample without nanometals and also without grape extract, which was characterized by a smooth surface, low color and odor intensity, higher stickiness, and flexibility, also differed significantly. As reported by Marvizadeh et al. [24], increasing the proportion of zinc and titanium oxide nanoparticles caused a decrease in the flexibility of edible packaging, however, the packaging showed a smooth surface without pores or cracks. For the samples analyzed in this study, the flexibility values of the samples containing nanometals, but without the added grape extract, showed rather higher flexibility compared to the control sample. Surface roughness ranged from 1.89 to 8.49. As reported by Marvizadeh et al. [24], the addition of nanometals also contributed to a change in the instrumentally-determined color in the CIELab system by a significant reduction in values of  $L$  and at the same time increase in values of  $a^*$  and  $b^*$ , which showed a slight reddish and yellowish tinge. In our study, the color intensity of the packages was sensory evaluated, which was in most samples without grape extract also slightly higher compared to the control sample.

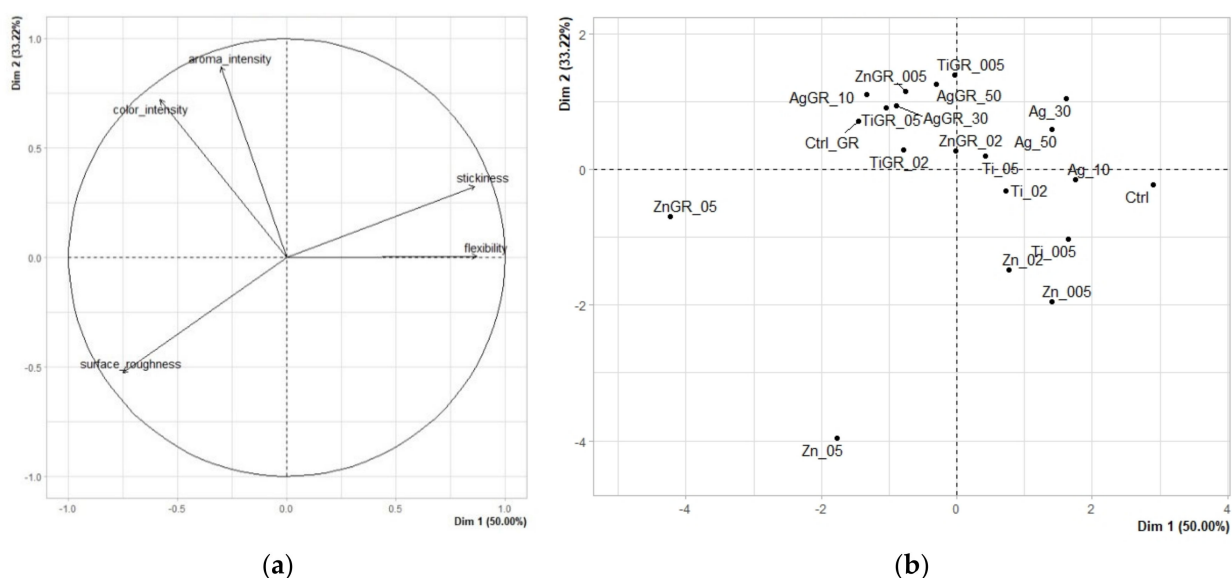


**Figure 1.** The PCA results of quantitative descriptive analysis of edible coatings: (a) Variables factor map. (b) Score plot for the mean points.

### 3.1.2. Hedonic Analysis

A total of 11 samples, that were already evaluated by the panel in the previous step and reached the overall average score higher than 5 and were therefore evaluated as sensory acceptable, were afterward analyzed hedonically by untrained evaluators.

Factor analysis (Figure 2a) confirmed a close correlation between overall evaluation and appearance pleasantness, and to a lesser extent also odor pleasantness. The principal

component analysis results graph explains 99.31% variability using the two principal components, with the first component explaining 93.31% and the second component only 6.00% variability. From the sample map (Figure 2b) and from Table 3 showing statistically significant ( $p < 0.05$ ) differences between individual edible films, it can be seen that there were a number of statistically significant differences between individual edible packaging samples.

**Table 2.** Adjusted mean values of evaluation within the quantitative descriptive analysis of edible packaging.

	Flexibility	Stickiness	Aroma Intensity	Color Intensity	Surface Roughness
Ctrl	8.041	4.625	3.636	2.618	2.986
Ag_10	8.005	3.630	4.216	3.158	2.592
Ti_005	7.605	3.830	3.416	3.658	3.592
Ag_30	8.205	4.330	5.216	4.458	3.092
Zn_005	6.705	3.330	3.016	1.858	3.592
Ag_50	8.705	4.330	4.616	5.858	4.092
Zn_02	7.705	2.830	3.916	2.058	4.492
Ti_02	7.905	3.13	3.716	6.358	3.492
Ti_05	7.605	3.13	4.116	6.758	3.592
ZnGR_02	7.705	2.73	4.616	6.558	3.992
TiGR_005	4.405	3.43	4.616	7.958	1.892
AgGR_50	5.205	3.33	4.816	8.958	3.192
ZnGR_005	4.905	3.13	4.916	7.658	3.492
TiGR_02	6.605	2.93	4.416	8.558	5.192
AgGR_30	4.305	3.33	4.616	8.658	3.892
TiGR_05	6.305	2.73	5.116	8.558	4.792
Zn_05	4.005	2.03	2.516	2.858	8.392
CtrlGR	3.405	3.13	4.816	7.758	4.292
AgGR_10	4.605	3.23	5.416	8.058	4.692
ZnGR_05	1.705	1.63	5.316	7.358	8.492

Values highlighted with green color are statistically significantly higher, values highlighted with orange color are statistically significantly lower ( $p < 0.05$ ).

The remote sample Ag\_50, characterized by the lowest values of pleasantness in all evaluated descriptors, was clearly singled out on the sample map. The second remote and worst-rated sample was Ti\_05. The best evaluated was the control sample without nanometals and grape extract, which, however, was closely followed by samples with ZnO nanoparticles in concentrations of 0.2 and 0.05%. All these samples achieved low values in color and odor intensity and were characterized by a smooth surface with high flexibility. Thus, the high scores in the overall rating were related to their neutral nature, which is preferred for edible packaging [25,26]. Thus, samples without grape extract generally reached higher values, however, the ZnGR\_02 sample achieved average values and was evaluated as generally acceptable.

The addition of nanometals is important from a functional point of view and enables the production of packaging with antimicrobial activity [27]. However, samples with a higher concentration of nanometal addition generally achieved lower pleasantness.

### 3.1.3. Assessment of the Probability of Purchasing Food Commodities in Edible Packaging

The results of the analysis showing how probable it is that different groups of food commodities packed in individual edible coatings will be purchased are shown in Table 4. As most of the values were below 3, it is clear that the evaluators could not imagine the use of the analyzed edible packaging for commodity groups such as meat products, milk products (cheeses), bakery products, or fruit and vegetables. The highest values, i.e., the highest probability of food purchase, were achieved by the control sample not containing grape extract or nanometals. Of the samples containing nanometals, the use of samples with 0.05% and 0.2% concentration of ZnO nanoparticles was the most conceivable for the

evaluators for all evaluated types of commodities, and the Ti\_005 sample for the packaging of fruit, vegetables, and milk products.

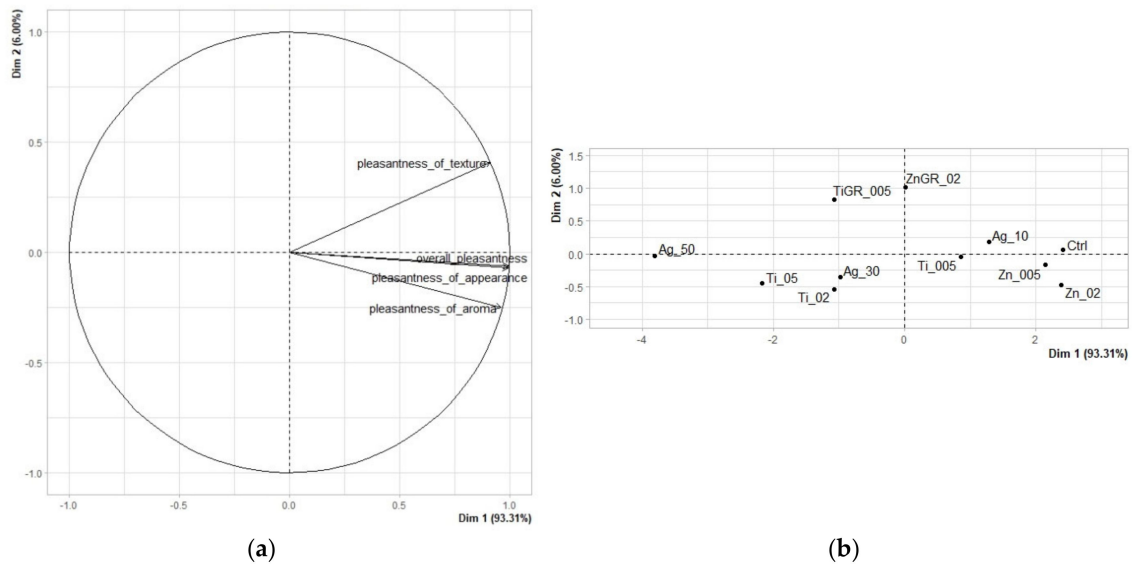


**Figure 2.** The PCA results of hedonic analysis of edible coatings: (a) Variables factor map. (b) Score plot for the mean points.

**Table 3.** Adjusted mean scores of hedonic evaluation of edible coatings.

	Texture Pleasantness	Aroma Pleasantness	Appearance Pleasantness	Overall Pleasantness
Ag_50	5.800	4.708	3.031	4.569
Ti_05	6.000	5.123	4.185	5.262
TiGR_005	6.677	5.031	4.785	5.708
Ti_02	6.215	5.385	4.815	5.723
Ag_30	6.308	5.369	4.785	5.769
ZnGR_02	7.031	5.308	5.215	6.000
Ti_005	6.754	5.538	6.262	6.723
Ag_10	6.954	5.631	6.415	6.769
Zn_005	6.985	5.815	7.138	7.262
Zn_02	6.938	5.954	7.323	7.323
Ctrl	7.169	5.908	7.031	7.246

Values highlighted with green color are statistically significantly higher, values highlighted with orange color are statistically significantly lower ( $p > 0.05$ ).

**Table 4.** Adjusted mean scores of the probability of purchasing a certain commodity in an edible coating.

	Meat Products	Milk Products (Cheese)	Bakery Products	Fruit	Vegetables
Ag_50	1.865	1.676	1.703	1.595	1.595
ZnGR_02	3.081	2.027	2.270	2.189	2.162
Ti_05	2.351	3.351	2.081	2.162	2.162
TiGR_005	3.459	1.946	2.162	2.243	2.081
Ag_30	2.676	2.324	2.514	2.432	2.405
Ti_02	2.270	3.378	2.351	2.514	2.459
Ag_10	2.946	2.784	2.649	2.919	3.000
Ti_005	2.973	3.405	2.973	3.216	3.270
Ctrl	3.000	3.405	2.649	3.676	3.459
Zn_02	3.703	3.595	3.378	4.000	3.838
Zn_005	3.730	3.811	3.432	4.324	4.297

Values highlighted with green color are statistically significantly higher, values highlighted with orange color are statistically significantly lower ( $p > 0.05$ ).

### 3.2. Evaluation of Color and Color Properties of Packaging

Digital images of individual samples of edible packaging with the addition of Ag, TiO<sub>2</sub>, ZnO nanoparticles, and red grape extract are shown in Figures 3–5. The results of the evaluation of individual color properties of packaging are summarized in Table 5, no statistically significant difference was found for samples with the same letter.

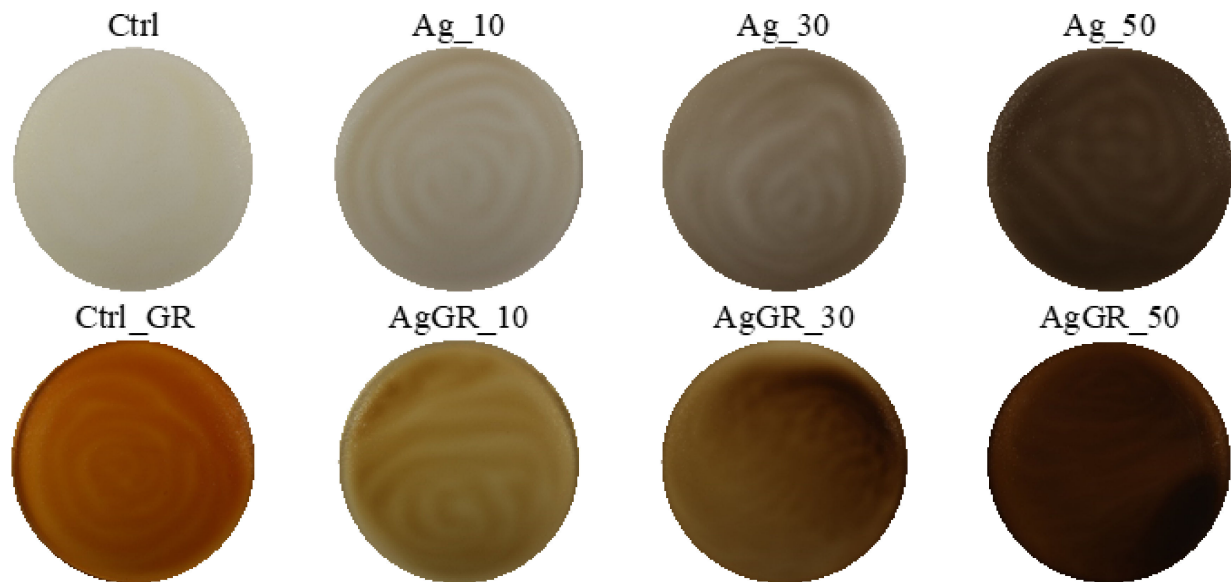


**Figure 3.** Digital images of edible coatings used for color analysis—samples with the addition of Ag nanoparticles.

The samples with the addition of silver showed a decrease in the parameter compared to the control samples (Ctrl and Ctrl\_GR)  $L^*$ , on the contrary, there was an increase for parameters  $a^*$  and  $b^*$  (depending on the concentration added).

A comparison of the differences ( $\Delta E$ ) of samples in individual groups from the control samples Ctrl and Ctrl\_GR is shown in Figure 6a. A statistically significant difference ( $p < 0.05$ ) was demonstrated when comparing the measurement results and the calculated  $\Delta E$  parameter. As the concentration of Ag and ZnO nanoparticles addition was increased, the difference ( $\Delta E$ ) between the samples and the control sample without the addition of grape extract clearly increased as well. However, in the case of samples containing grape extract, this clear trend was only confirmed in the case of the addition of TiO<sub>2</sub> nanoparticles.

In addition, the reduction in lightness (L) can be attributed to the opacity of the silver nanoparticles [11]. According to a study by Rhim et al. (2013) who monitored the effect of the addition of silver nanoparticles, the parameter  $\Delta E$  increases, and the color of the packaging changes to dark brown depending on the concentration of silver nanoparticles [28]. We achieved similar results in our study.

For packaging samples with the addition of TiO<sub>2</sub> nanoparticles,  $\Delta E$  increased, which is in line with the results of a similar study by Dash et al. (2019) [29]. Coatings containing TiO<sub>2</sub> should also have a higher parameter of  $L^*$ ,  $b^*$ , and  $\Delta E$  with increasing concentration [30]. Our study delivered corresponding values.

In their work, Wardana et al. (2018) reported that increasing the addition of ZnO nanoparticles increases  $\Delta E$ , which corresponds to our results [31].



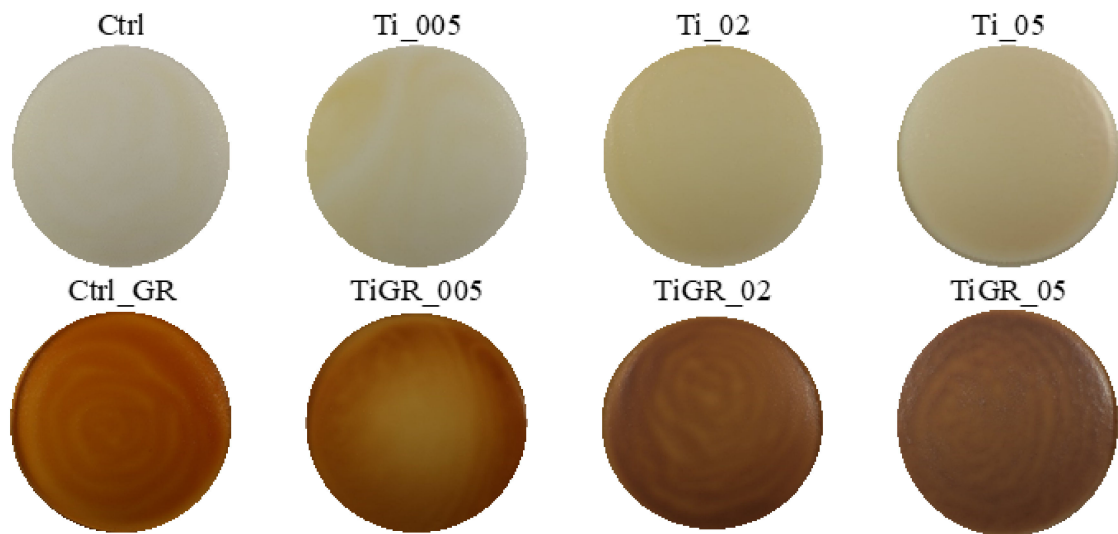


**Figure 4.** Digital images of edible coatings used for color analysis—samples with added TiO<sub>2</sub> nanoparticles.

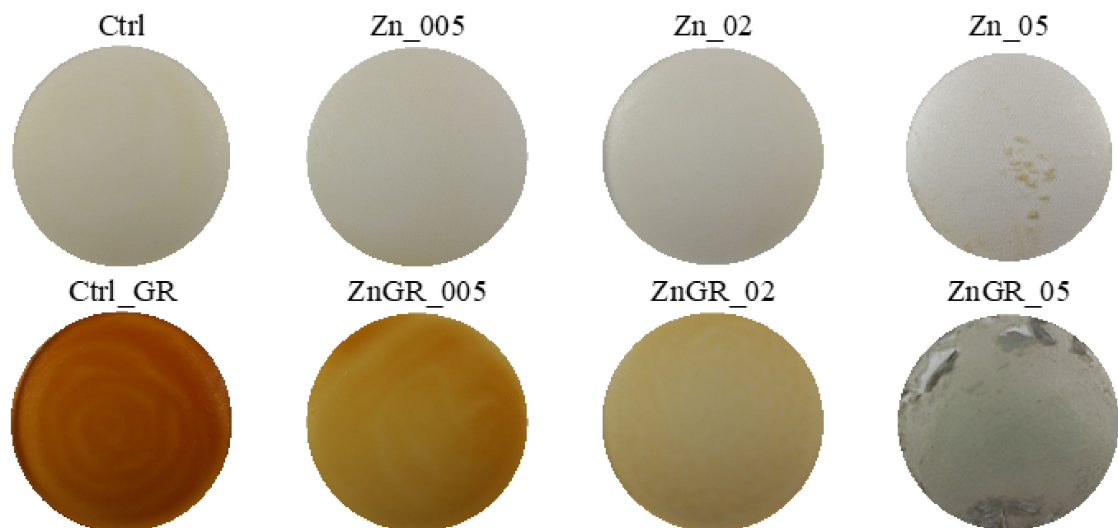


**Figure 5.** Digital images of edible coatings used for color analysis—samples with the addition of ZnO nanoparticles.

### 3.2.1. Opacity

A comparison of differences in the transparency of packaging, which was calculated from the L value obtained from images against a white and a black background, is shown in Figure 6b.

The lowest opacity values were reached by the control samples (Ctrl and Ctrl\_GR). All other samples had a higher value, which increased with increasing concentration. As a result, the samples were less transparent. The transparency of the packaging, therefore, decreased with increasing concentrations. This trend was clear both for samples with and without grape extract. Individual results are summarized in Table 5, no statistically significant difference was found for samples with the same letter.

**Table 5.** Results of evaluation of color properties of packaging.

	$L^*$	$a^*$	$b^*$	$\Delta E$	Opacity	Whiteness Index	Yellowness Index
Ag_10	56.15 ± 0.21	0.56 ± 0.04	11.90 ± 0.08	9.63 ± 0.31 <sup>l</sup>	17.57 ± 0.37	54.56 ± 0.20	30.28 ± 0.21
Ag_30	41.36 ± 0.18	2.66 ± 0.02	13.44 ± 0.09	25.11 ± 0.36	26.11 ± 0.47	39.78 ± 0.16	46.43 ± 0.16 <sup>v</sup>
Ag_50	17.19 ± 0.24	5.43 ± 0.05 <sup>e</sup>	12.76 ± 0.09	45.88 ± 0.41	66.86 ± 1.67	16.04 ± 0.22 <sup>t</sup>	106.09 ± 0.87
AgGR_10	42.26 ± 0.28	5.33 ± 0.12 <sup>e</sup>	35.58 ± 0.15	15.57 ± 0.17	12.95 ± 0.13 <sup>o</sup>	31.97 ± 0.17	120.29 ± 0.45
AgGR_30	24.11 ± 0.45	10.32 ± 0.24 <sup>f</sup>	26.30 ± 0.16	12.43 ± 0.23	21.23 ± 1.03	19.02 ± 0.42	155.93 ± 2.38
AgGR_50	9.06 ± 0.20	10.45 ± 0.14 <sup>f</sup>	11.32 ± 0.30 <sup>s</sup>	23.04 ± 0.40	45.35 ± 1.27	7.76 ± 0.14	178.45 ± 0.99
Ti_005	64.66 ± 0.25 <sup>a</sup>	−2.20 ± 0.12 <sup>d</sup>	17.12 ± 0.24	3.91 ± 0.13 <sup>i</sup>	32.42 ± 0.32	60.67 ± 0.26	37.82 ± 0.56
Ti_02	63.41 ± 0.28	−1.76 ± 0.05	24.51 ± 0.09	7.75 ± 0.18 <sup>k</sup>	70.54 ± 0.49	55.92 ± 0.26	55.23 ± 0.40
Ti_05	64.27 ± 0.36 <sup>a</sup>	−0.51 ± 0.02	20.96 ± 0.09 <sup>h</sup>	6.05 ± 0.20 <sup>j</sup>	86.48 ± 0.85	58.57 ± 0.35	46.60 ± 0.44 <sup>v</sup>
TiGR_005	35.16 ± 0.30	17.93 ± 0.08	40.17 ± 0.23	5.37 ± 0.07	16.03 ± 0.35 <sup>s</sup>	21.64 ± 0.13 <sup>u</sup>	163.22 ± 0.47
TiGR_02	30.62 ± 0.26	16.42 ± 0.05	26.91 ± 0.11	7.54 ± 0.27 <sup>k</sup>	62.91 ± 1.01	23.80 ± 0.20	125.55 ± 0.59
TiGR_05	33.41 ± 0.31 <sup>b</sup>	13.46 ± 0.07	21.08 ± 0.13 <sup>h</sup>	9.85 ± 0.11 <sup>l</sup>	81.05 ± 0.96	28.87 ± 0.26 <sup>u</sup>	90.14 ± 0.60
Zn_005	68.42 ± 0.36	−1.07 ± 0.05	8.03 ± 0.05	2.75 ± 0.25	14.65 ± 0.22 <sup>qr</sup>	67.39 ± 0.34	16.78 ± 0.16
Zn_02	68.66 ± 0.39 <sup>c</sup>	−0.82 ± 0.08	6.52 ± 0.09	3.88 ± 0.17 <sup>i</sup>	15.01 ± 0.29 <sup>prs</sup>	67.98 ± 0.40	13.56 ± 0.25
Zn_05	70.33 ± 0.42 <sup>c</sup>	−0.28 ± 0.03	4.38 ± 0.10	6.05 ± 0.22 <sup>j</sup>	24.06 ± 0.76	70.01 ± 0.42	8.90 ± 0.23
ZnGR_005	47.00 ± 0.35	10.09 ± 0.15	46.77 ± 0.20	16.70 ± 0.45	8.38 ± 0.18 <sup>n</sup>	28.60 ± 0.20	142.17 ± 0.70
ZnGR_02	57.89 ± 0.42	0.16 ± 0.10	28.16 ± 0.09	29.09 ± 0.49 <sup>m</sup>	10.45 ± 0.20	49.34 ± 0.32	69.50 ± 0.42
ZnGR_05	52.11 ± 0.35	−2.08 ± 0.04 <sup>d</sup>	7.70 ± 0.06	28.67 ± 0.29 <sup>m</sup>	89.04 ± 0.82	51.45 ± 0.35	21.11 ± 0.25
Ctrl	66.91 ± 0.37	−1.41 ± 0.03	11.54 ± 0.10 <sup>s</sup>	-	14.13 ± 0.55 <sup>opq</sup>	64.93 ± 0.40	24.63 ± 0.32
Ctrl_GR	33.89 ± 0.43 <sup>a</sup>	27.49 ± 0.18	43.91 ± 0.34	-	7.59 ± 0.20 <sup>n</sup>	16.01 ± 0.16 <sup>t</sup>	185.12 ± 0.96

\* Samples marked with indices within the column do not differ statistically significantly from each other.

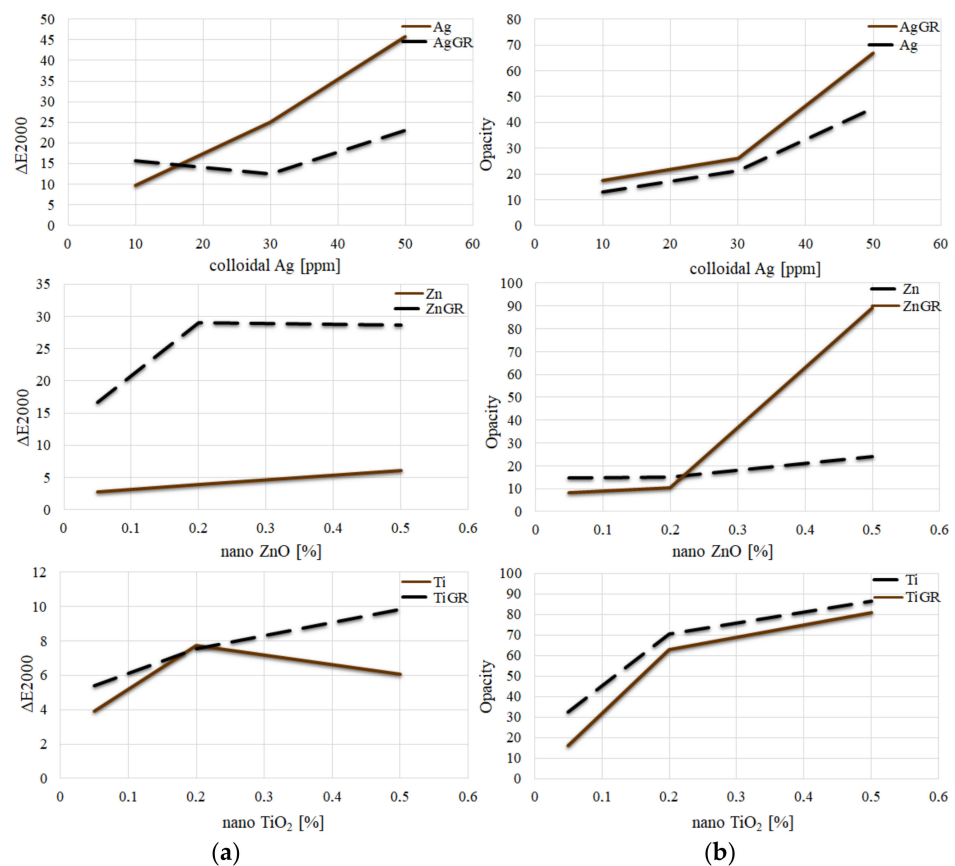


**Figure 6.** Evaluation of color properties of packaging: (a) A comparison of differences ( $\Delta E$ ) of the samples in individual groups from the control sample Ctrl/Ctrl\_GR. (b) Comparison of sample opacity with individual additions.

### 3.2.2. Whiteness Index; Yellowness Index

Samples containing 10% grape addition had a lower Whiteness Index than samples without the additive. In their study, Li et al. (2019) report that the reduction in whiteness is probably due to the formation of dark compounds formed during the Maillard reaction [20]. In the case of the addition of Ag nanoparticles, the Whiteness Index decreased with increasing concentrations, regardless of the addition of grape extract. The addition of ZnO and TiO<sub>2</sub> nanoparticles increased the Whiteness Index values rather slightly, which is consistent with the results in a study by Dash et al. (2019) [29]. Coatings containing TiO<sub>2</sub> should also have higher parameters of  $L^*$ ,  $b^*$ ,  $\Delta E$ , as well as Whiteness Index, with increasing concentration [30]. We achieved similar results in our study.

Samples with the addition of grape extract generally had a higher Yellowness Index than samples without this additive. In the case of the addition of Ag nanoparticles, the Yellowness Index increased with increasing concentrations, regardless of the addition of grape extract. On the contrary, the addition of ZnO and TiO<sub>2</sub> nanoparticles rather reduced the values of the Yellowness Index (Figure 7).

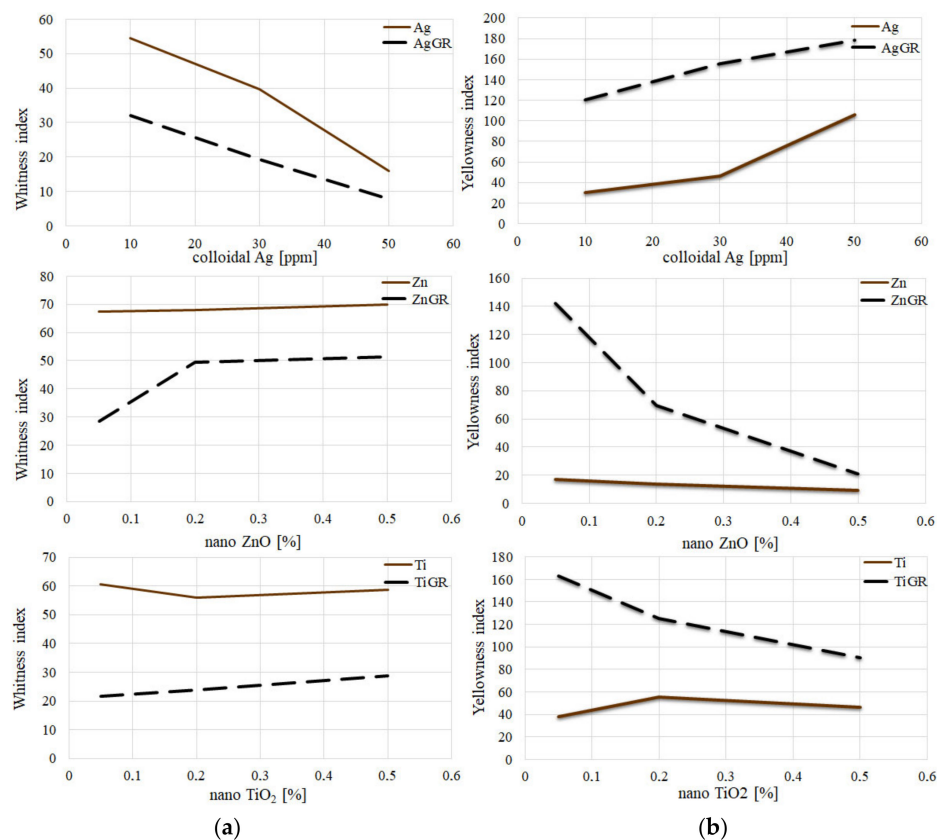


**Figure 7.** Evaluation of color properties of packaging: (a) Comparison of Whiteness Index with individual additions. (b) Comparison of Yellowness Index with individual additions.

### 3.3. Evaluation of the Surface of Edible Packaging

The comparison of the Ctrl control and the Ctrl\_GR containing grape extract shows a minimum difference. At Ctrl\_GR, there is a small occurrence of insoluble particles of grape extracts confirmed both, on the surface as well as in the cracks (Figure 8 Ctrl\_GR). The insoluble matter distribution is random and there is no separation of thermodynamic phases. The total number of cracks and the distance between the cracks were the lowest in the control samples, and statistical differences between the control and other samples were confirmed ( $p < 0.05$ ) (Tables 6 and 7). The difference in comparison with the control containing the addition of the grape extract was not proved at the nearest object distance

in ZnGr\_005, the difference was not confirmed in the sample with the addition of grape extract in ZnGR\_02.

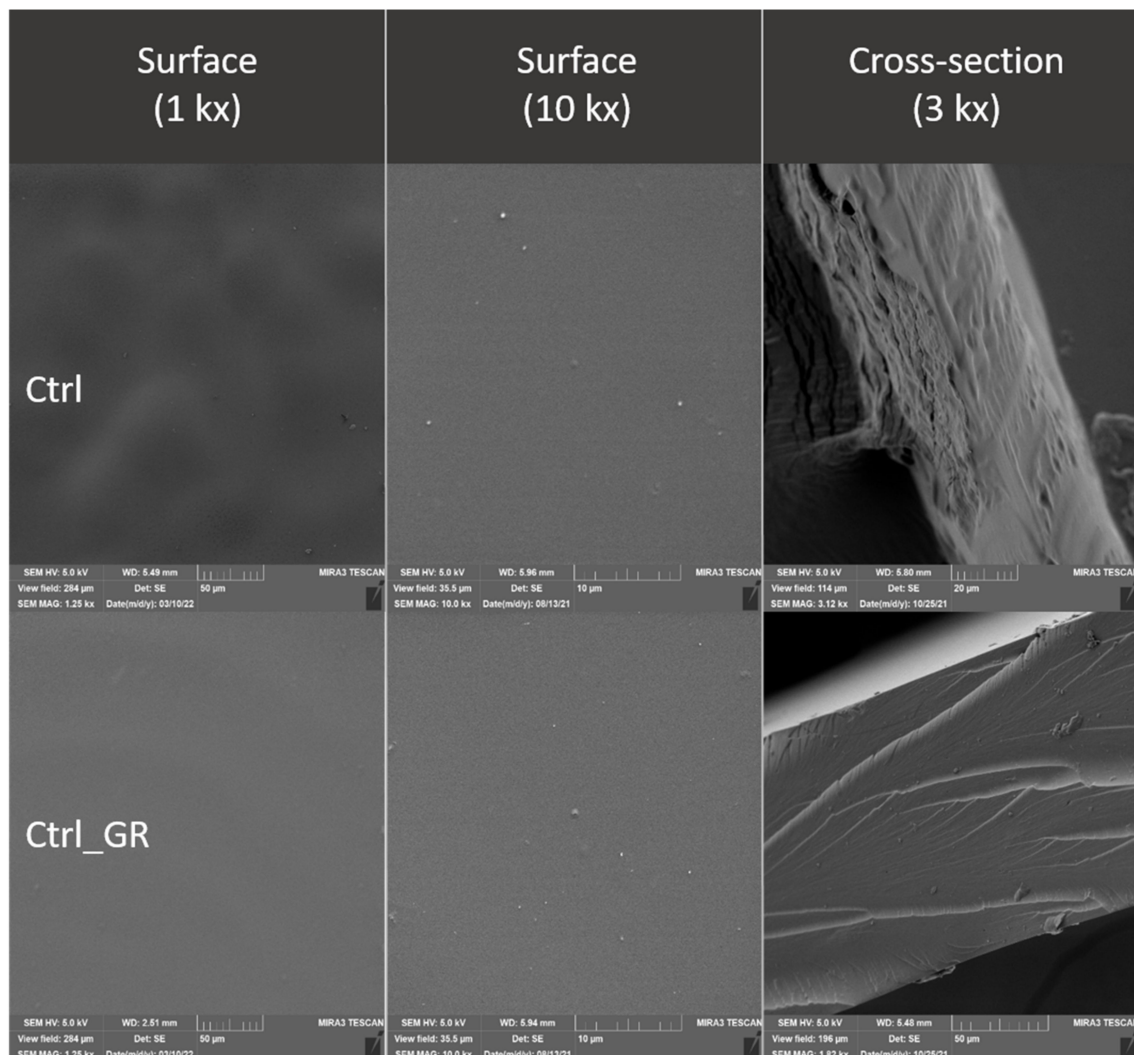


**Figure 8.** Surface and fracture microstructure of control samples of edible packaging.

As concluded by Bakhy et al. (2018), metal oxide nanoparticles, such as nano-Ag, improve the mechanical and barrier properties of biodegradable films [32]. Colloidal silver, like other nanoparticles, forms structures that roughen the surface or are visible at cracks. The silver distribution is uneven and strongly adheres to the chitosan gel [33]. Many authors describe the shape characteristics of nanosilver differently, when they even state the size of silver 80–110 nm, i.e., above the well-known term of nanoparticles (max 100 nm). In the case of our study, the presence of colloidal silver was not confirmed (Figures 9 and 10). However, the addition affected the nearest object distance when there was a statistically significant decrease in the concentration of Ag30 and AgHr30 ( $p < 0.05$ ). For the area, this phenomenon was confirmed only for samples without added extract (Tables 6 and 7).

The microstructure of the surface of edible coatings was also observed after the addition of  $\text{TiO}_2$  (Figures 11 and 12). As several authors claim,  $\text{TiO}_2$  forms polygonal and oval crystals with an average size of 1.84–40  $\mu\text{m}$  [32]. Our results also confirmed the oval shape of  $\text{TiO}_2$  crystals. Crystal formation was observed on the surface, but also in the fractures of the packaging. This result is partly consistent with [34], where they confirmed the formation of crystals only in the fractures, while they were not observed on the surface. The difference may be due to the different concentrations, where a uniform

concentration of 1% TiO<sub>2</sub> was used in this study, however, the concentrations in our study were lower, namely 0.05–0.5%. Many authors confirm the properties we observed, when crystal formation occurs in the entire range of biodegradable films [35]. From the fissure area comparison, no statistical difference was confirmed for samples from Ti\_005 and 02 concentrations ( $p > 0.05$ ), the concentration with the highest Ti\_05 addition was statistically different ( $p < 0.05$ ) (Table 7). The nearest object distance was different between samples in all cases ( $p < 0.05$ ) (Table 6).

**Table 6.** Nearest object distance between fissures.

Sample	Nearest Object Distance (nm)	Sample	Nearest Object Distance (nm)
Ctrl	38.25 ± 23.12 <sup>a</sup>	Ctrl	43.95 ± 23.77 <sup>a</sup>
Ag_10	68.49 ± 25.32 <sup>b</sup>	AgGR_10	61.42 ± 23.95 <sup>b</sup>
Ag_30	54.27 ± 24.63 <sup>c</sup>	AgGR_30	57.56 ± 24.26 <sup>c</sup>
Ag_50	62.95 ± 24.77 <sup>d</sup>	AgGR_50	62.86 ± 23.42 <sup>d</sup>
Ti_005	46.11 ± 19.93 <sup>e</sup>	TiGR_005	50.18 ± 23.86 <sup>e</sup>
Ti_02	55.7 ± 24.56 <sup>f</sup>	TiGR_02	49.46 ± 23.84 <sup>f</sup>
Ti_05	63.26 ± 25.09 <sup>g</sup>	TiGR_05	45.84 ± 23.76 <sup>g</sup>
Zn_005	46.49 ± 24.07 <sup>h</sup>	ZnGR_005	43.48 ± 23.2 <sup>a</sup>
Zn_02	33.54 ± 27.62 <sup>e</sup>	ZnGR_02	40.36 ± 21.63 <sup>h</sup>
Zn_05	43.48 ± 23.2 <sup>i</sup>	ZnGR_05	93.06 ± 31.52 <sup>i</sup>

**Table 7.** Total fissure area.

Sample	Area (µm <sup>2</sup> )	Sample	Area (µm <sup>2</sup> )
Ctrl	0.52 ± 1.53 <sup>a</sup>	Ctrl	1.04 ± 3.72 <sup>a</sup>
Ag_10	1.97 ± 3.47 <sup>b</sup>	AgGR_10	1.12 ± 1.65 <sup>b</sup>
Ag_30	1.5 ± 2.89 <sup>c</sup>	AgGR_30	1.55 ± 3.08 <sup>c</sup>
Ag_50	1.82 ± 3.87 <sup>d</sup>	AgGR_50	1.54 ± 2.94 <sup>d</sup>
Ti_005	1.77 ± 14.22 <sup>e</sup>	TiGR_005	1.71 ± 4.13 <sup>e</sup>
Ti_02	1.67 ± 3.95 <sup>e</sup>	TiGR_02	1.97 ± 5.78 <sup>e</sup>
Ti_05	0.97 ± 1.47 <sup>f</sup>	TiGR_05	1.41 ± 4 <sup>f</sup>
Zn_005	1.66 ± 6.02 <sup>g</sup>	ZnGR_005	1.31 ± 3.69 <sup>g</sup>
Zn_02	0.99 ± 1.93 <sup>g</sup>	ZnGR_02	0.6 ± 6 <sup>a</sup>
Zn_05	0.35 ± 3.65 <sup>h</sup>	ZnGR_05	6.67 ± 6.59 <sup>h</sup>

The addition of ZnO to edible package resulted in a roughening of the surface of the package in comparison with the control (Figure 9, Figure 13, and Figure 14). From the point of view of the microstructure, ZnO particles have a regular circular structure [5] which was also reflected in the structure of the formed edible packaging. Similar findings are also confirmed by other studies, where ZnO also formed an irregular structure visible in SEM, from the addition of 0.1–1.0% upwards [5]. At a higher magnification, the circular structure of ZnO projected on the surface was visible. In some cases, other structures may be formed, such as crystalline efflorescence [20]. Crystalline efflorescence was confirmed in this study, especially on the surface of the packaging. Crystal formation was accompanied by phase segregation, which was caused by thermodynamic incompatibilities commonly described in biofilms [36]. In the case of Zn and ZnGR samples at concentrations of 0.2–0.5%, cracks breaking the surface of the edible coating were also observed. The origin of the cracks was due to the different thermodynamic properties of the two materials. Crystals and phase segregations were observed in the ZnGR 0.05 and 0.2% samples at the fracture. The ZnGR\_05 sample was characterized by large uneven crystals along with peeling parts due to phase segregation. The particle distribution was uneven on the surface as well as in the fracture of the package, which is in agreement with the results of other studies [5,37]. Uneven distribution was also confirmed by the largest nearest object distance and area in



samples with the addition of grape extract at the highest concentration of ZnHr05. ZnHr05 differed statistically from lower concentrations ( $p < 0.05$ ) (Tables 6 and 7, Figure 15). On the other hand, in samples without the addition of grape extract, the opposite connection was demonstrated in the area where ZnHr\_05 was the lowest. Nevertheless, at the nearest object distance, Zn\_02 was the lowest. These results indicate the randomness of crack formation within the edible films (Tables 6 and 7, Figures 13–15).

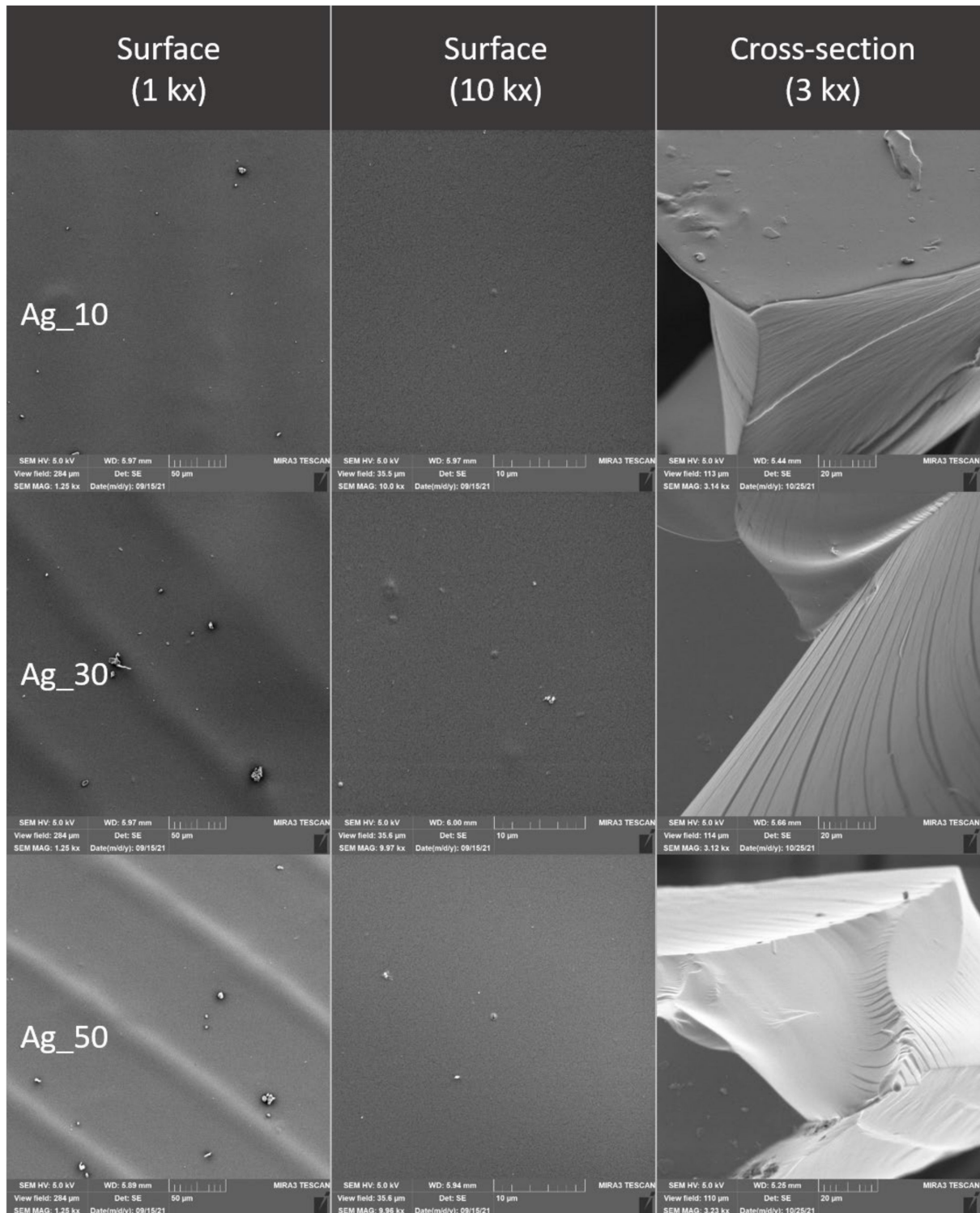


**Figure 9.** Surface and fracture microstructure of edible packaging with the addition of colloidal silver nanoparticles.

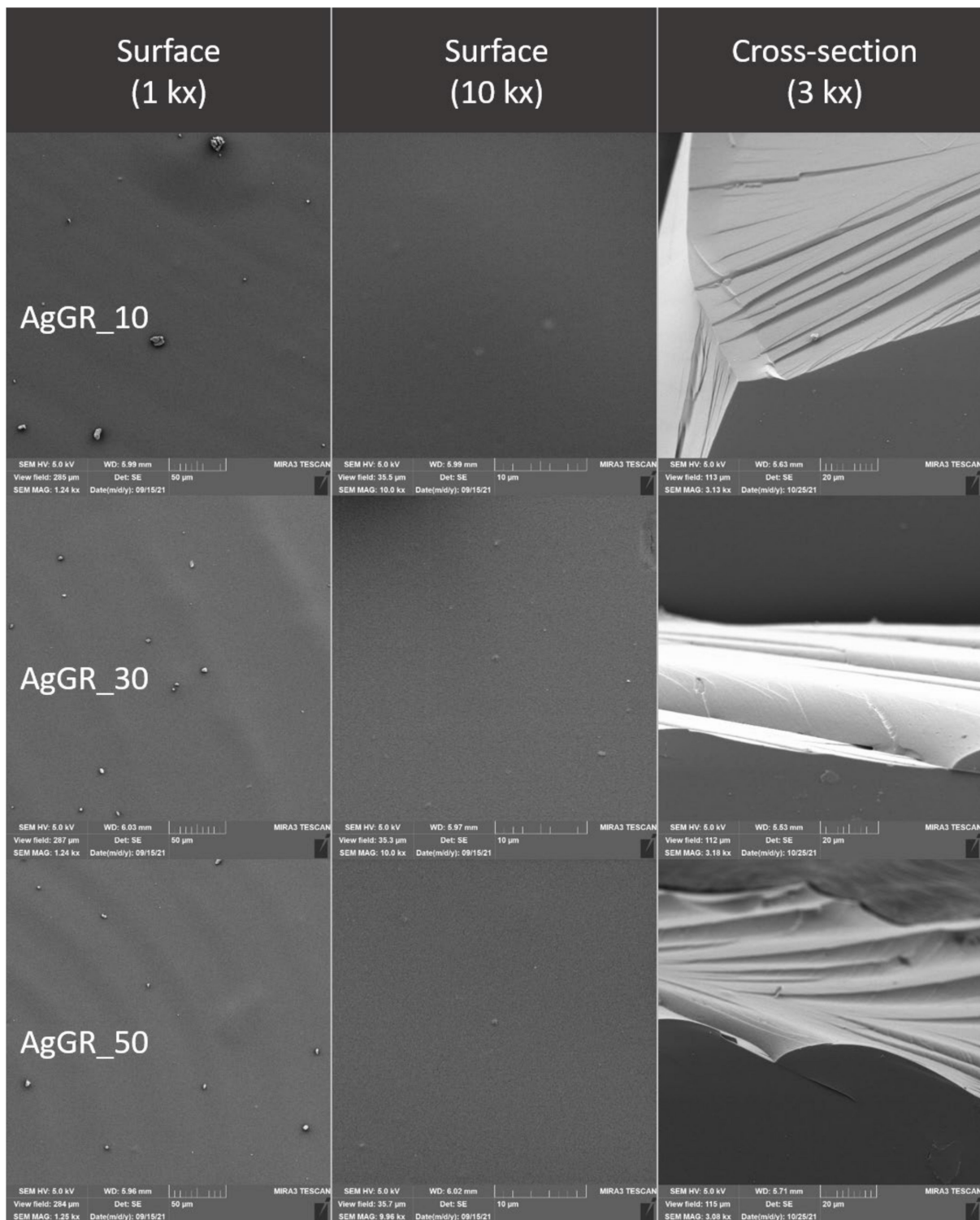


**Figure 10.** Surface and fracture microstructure of edible packaging with the addition of colloidal silver nanoparticles and grape extract.

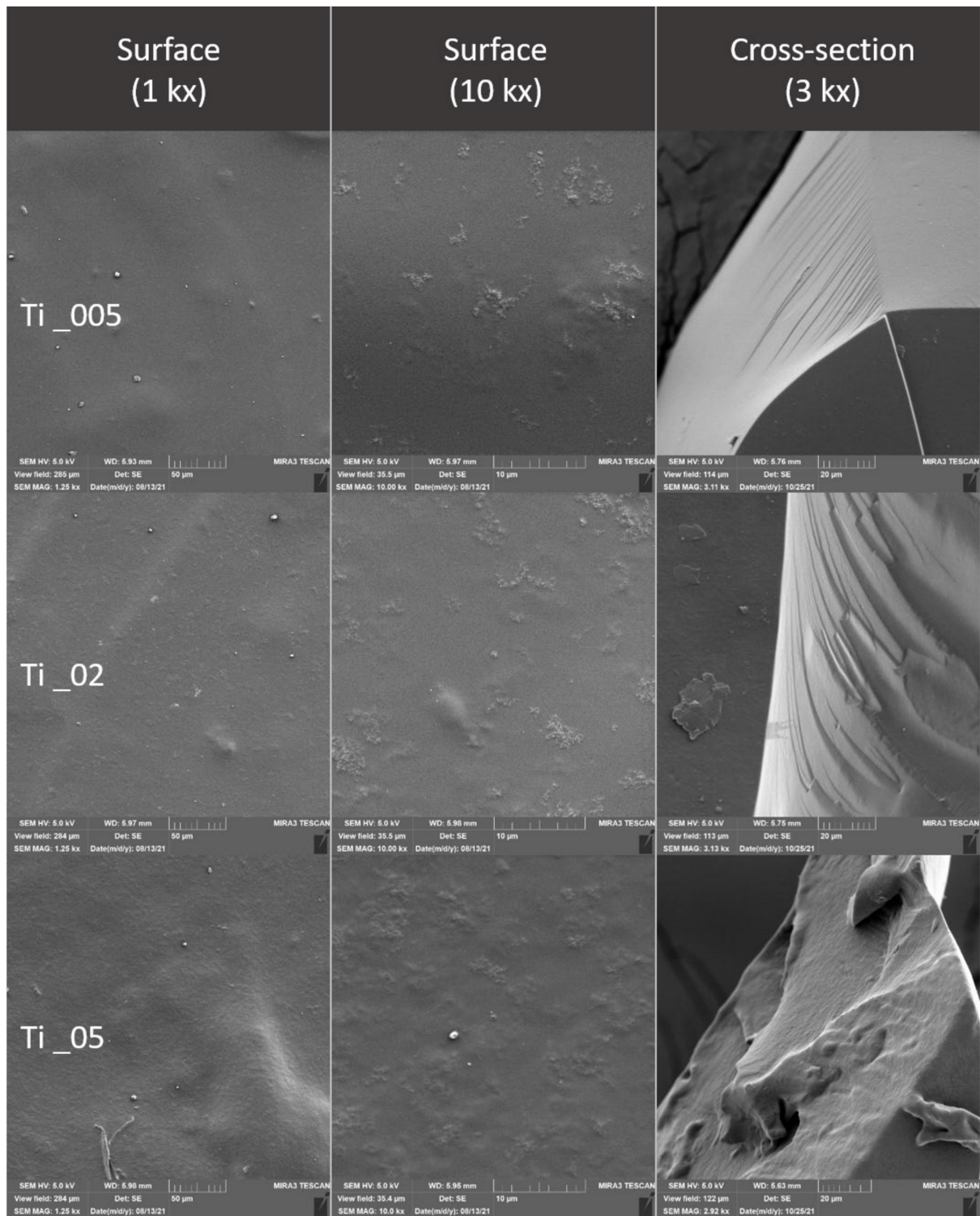


Figure 11. Surface and fracture microstructure of edible packaging with the addition of TiO<sub>2</sub> nanoparticles.



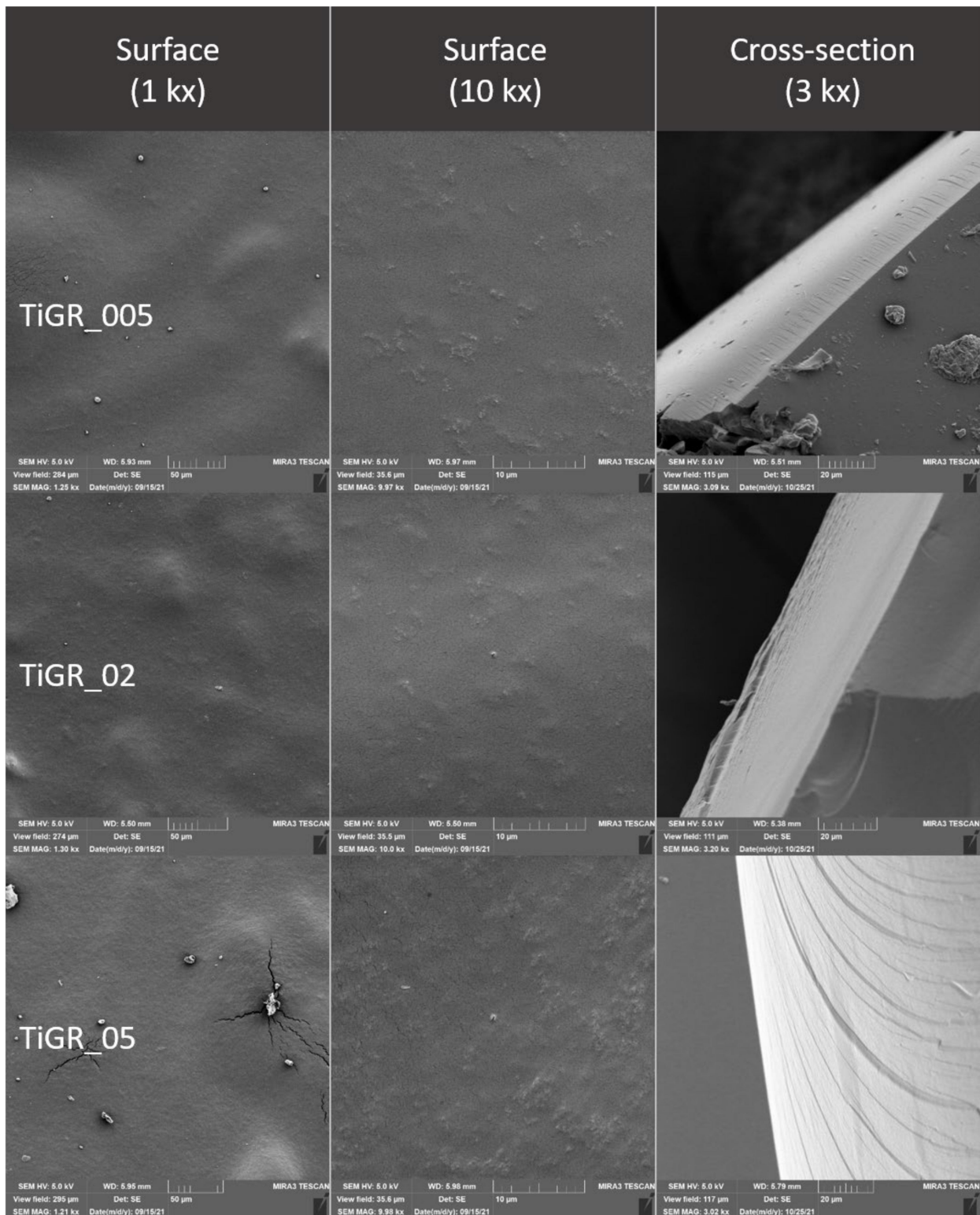


Figure 12. Surface and fracture microstructure of edible packaging with the addition of TiO<sub>2</sub> nanoparticles and grape extract.

Differences between samples with 10% grape extract and samples without the extract were confirmed in all samples examined. The presence of unspecified structures originating from the extraction process was confirmed in all samples of edible packaging containing the addition of grape extract. However, their incorporation into the chitosan network was confirmed, their presence caused a biofilm prominence, which is caused by the adherence of chitosan to plant tissues.

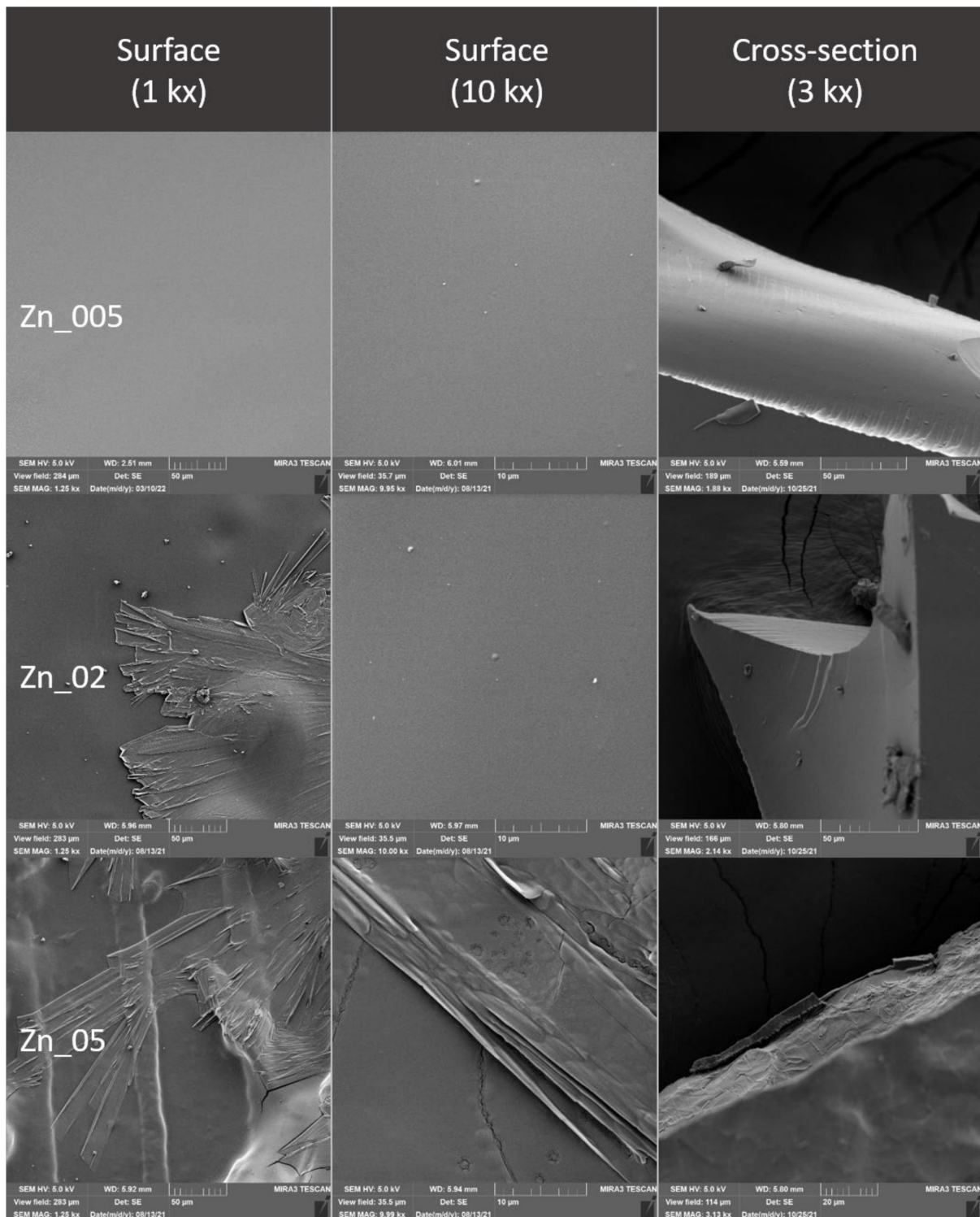
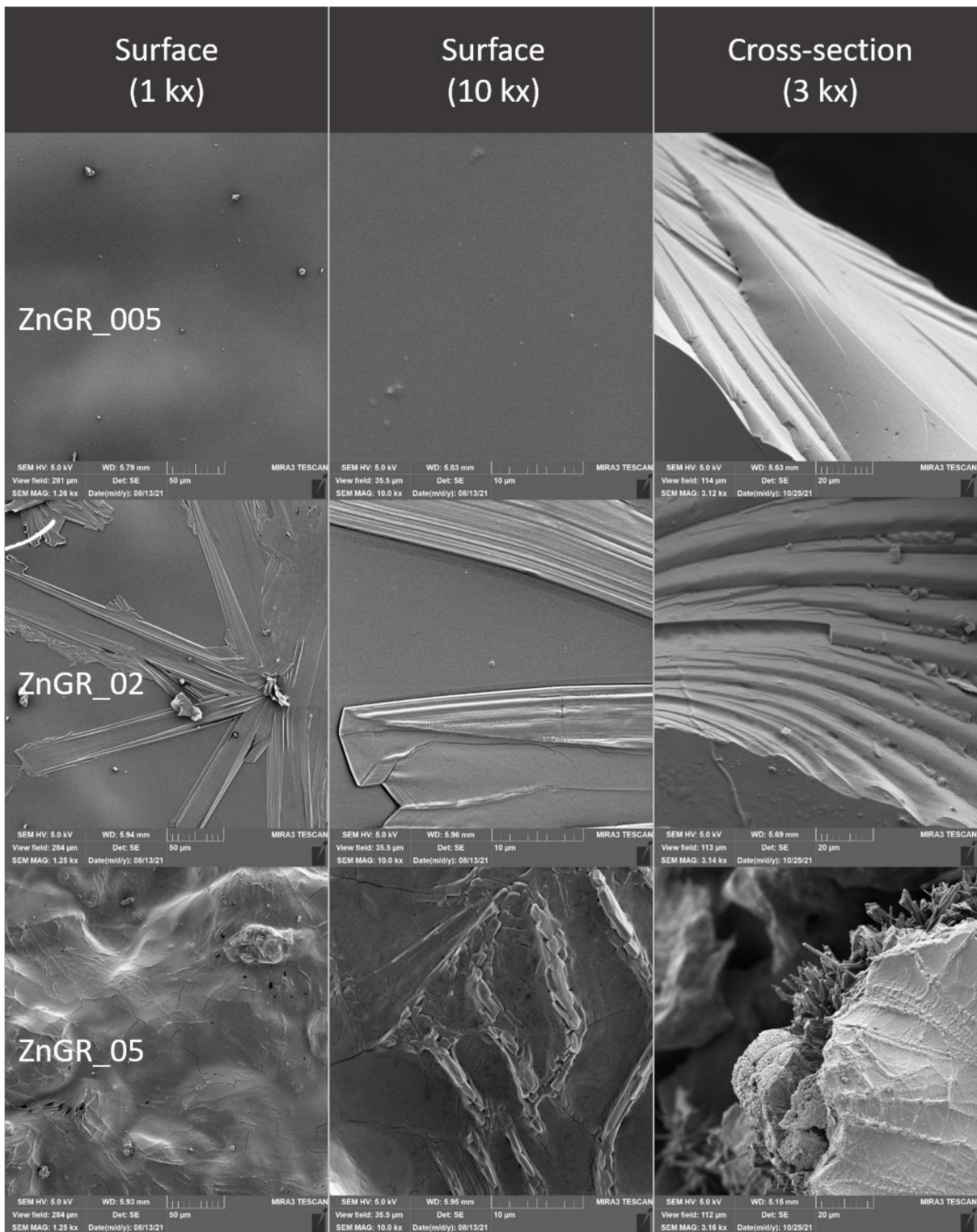


Figure 13. Surface and fracture microstructure of edible packaging with the addition of ZnO nanoparticles.





**Figure 14.** Surface and fracture microstructure of edible packaging with the addition of ZnO nanoparticles and grape extract.

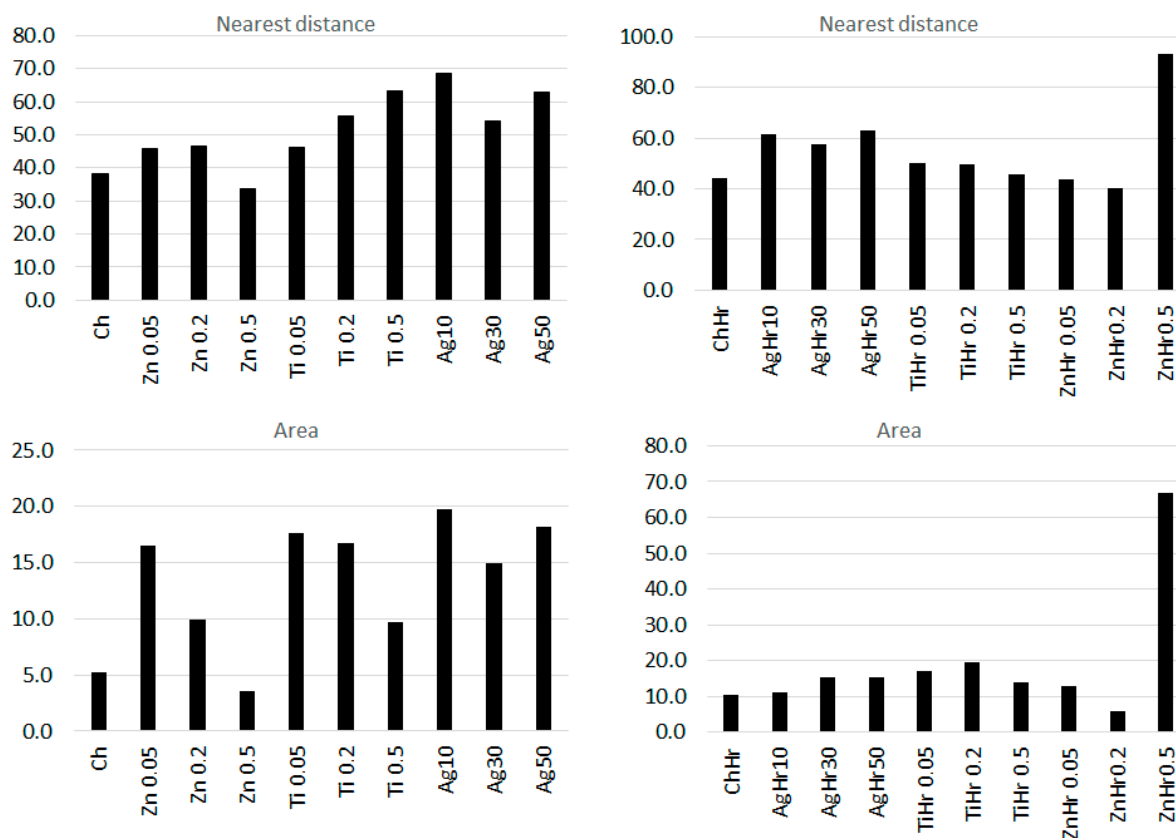


Figure 15. Comparison of the nearest object distance and area in edible films.

#### 4. Conclusions

The addition of grape extract generally reduced the flexibility of the samples and at the same time increased the intensity of odor and color to the extent that only two samples containing this extract and containing nanometals at the same time achieved a satisfactory score in the overall evaluation. There was no clear trend in terms of the effect of different nanometallic concentration additions on the quantitatively descriptively evaluated descriptors. However, the hedonic evaluation revealed that the addition of nanometals and their increasing concentration generally caused a deterioration in sample acceptability. In spite of that, the overall evaluation was higher than 5 in 9 out of the total number of 18 samples containing nanometals. From a sensory point of view, the addition of ZnO nanoparticles in concentrations of 0.05 and 0.2% appeared to be the most favorable of all nanometals.

The addition of nanometals also caused statistically significant changes in  $L^*$ ,  $a^*$ , and  $b^*$  values. The sample transparency generally decreased with increasing concentration of nanoparticle addition, regardless of the type of nanoparticle. The addition of grape extract significantly affected the samples in the Whiteness Index and Yellowness Index parameters, while the grape addition decreased the Whiteness Index values and increased the Yellowness Index values.

Electron microscopy also confirmed the differences between the control and the individual samples caused by the addition of nanometals, both on the basis of the evaluation of SEM images and on the basis of the evaluation of cracks in the formed edible film. The difference was not confirmed only between the control and the lowest concentrations for ZnGR\_005 for the nearest object distance and ZnGR\_02 for the area. The differences were confirmed on the surface and also in the fracture of edible chitosan-based packaging. Differences between samples with and without the addition of grape extract were also confirmed. In addition, our results confirmed that packaging handling causes structural

changes [15]. Therefore, for evaluation purposes, we recommend direct gel formation on a conductive target.

**Author Contributions:** Conceptualization, A.T., D.D. and B.T.; methodology, A.T., M.P. and Z.J.; validation, A.T., M.P., Z.J., D.D. and S.D.; formal analysis, A.T., M.P., Z.J., D.D., S.D. and K.T.; investigation, A.T., M.P., Z.J., D.D. and S.D.; resources, B.T.; data curation, D.D.; writing—original draft preparation, A.T., Z.J. and M.P.; writing—review and editing, H.K.M., A.T., B.T., D.D. and S.D.; visualization, A.T., H.K.M., Z.J. and M.P.; supervision, D.D. and B.T.; project administration, D.D.; funding acquisition, B.T. All authors have read and agreed to the published version of the manuscript.

**Funding:** This research was funded by ITA VETUNI, grant number 2021ITA24.

**Institutional Review Board Statement:** Not applicable.

**Informed Consent Statement:** Not applicable.

**Data Availability Statement:** Not applicable.

**Conflicts of Interest:** The authors declare no conflict of interest. The funders had no role in the design of the study; in the collection, analyses, or interpretation of data; in the writing of the manuscript; or in the decision to publish the results.

## References

- Zhang, W.; Zhang, Y.; Cao, J.; Jiang, W. Improving the Performance of Edible Food Packaging Films by Using Nanocellulose as an Additive. *Int. J. Biol. Macromol.* **2021**, *166*, 288–296. [[CrossRef](#)] [[PubMed](#)]
- Mohamed, S.A.A.; El-Sakhawy, M.; El-Sakhawy, M.A.-M. Polysaccharides, Protein and Lipid -Based Natural Edible Films in Food Packaging: A Review. *Carbohydr. Polym.* **2020**, *238*, 116178. [[CrossRef](#)] [[PubMed](#)]
- Darmajana, D.A.; Afifah, N.; Solihah, E.; Indriyanti, N. Effects of Carrageenan Edible Coating on Fresh Cut Melon Quality in Cold Storage. *Agritech* **2017**, *37*, 280–287. [[CrossRef](#)]
- Maringgal, B.; Hashim, N.; Tawakkal, I.S.M.A.; Mohamed, M.T.M. Recent Advance in Edible Coating and Its Effect on Fresh/Fresh-Cut Fruits Quality. *Trends Food Sci. Technol.* **2020**, *96*, 253–267. [[CrossRef](#)]
- La, D.D.; Nguyen-Tri, P.; Le, K.H.; Nguyen, P.T.M.; Nguyen, M.D.-B.; Vo, A.T.K.; Nguyen, M.T.H.; Chang, S.W.; Tran, L.D.; Chung, W.J.; et al. Effects of Antibacterial ZnO Nanoparticles on the Performance of a Chitosan/Gum Arabic Edible Coating for Post-Harvest Banana Preservation. *Prog. Org. Coat.* **2021**, *151*, 106057. [[CrossRef](#)]
- Bumbudsanpharoke, N.; Ko, S. Nano-Food Packaging: An Overview of Market, Migration Research, and Safety Regulations. *J. Food Sci.* **2015**, *80*, R910–R923. [[CrossRef](#)]
- Pushparaj, K.; Liu, W.-C.; Meyyazhagan, A.; Orlacchio, A.; Pappusamy, M.; Vadivalagan, C.; Robert, A.A.; Arumugam, V.A.; Kamyab, H.; Klemeš, J.J.; et al. Nano- from Nature to Nurture: A Comprehensive Review on Facets, Trends, Perspectives and Sustainability of Nanotechnology in the Food Sector. *Energy* **2022**, *240*, 122732. [[CrossRef](#)]
- Trajkowska Petkoska, A.; Daniloski, D.; D’Cunha, N.M.; Naumovski, N.; Broach, A.T. Edible Packaging: Sustainable Solutions and Novel Trends in Food Packaging. *Food Res. Int.* **2021**, *140*, 109981. [[CrossRef](#)]
- Alfei, S.; Marengo, B.; Zuccari, G. Nanotechnology Application in Food Packaging: A Plethora of Opportunities versus Pending Risks Assessment and Public Concerns. *Food Res. Int.* **2020**, *137*, 109664. [[CrossRef](#)]
- Kumar, S.; Basumatary, I.B.; Sudhani, H.P.K.; Bajpai, V.K.; Chen, L.; Shukla, S.; Mukherjee, A. Plant Extract Mediated Silver Nanoparticles and Their Applications as Antimicrobials and in Sustainable Food Packaging: A State-of-the-Art Review. *Trends Food Sci. Technol.* **2021**, *112*, 651–666. [[CrossRef](#)]
- Bahrami, A.; Mokarram, R.R.; Khiabani, M.S.; Ghanbarzadeh, B.; Salehi, R. Physico-Mechanical and Antimicrobial Properties of Tragacanth/Hydroxypropyl Methylcellulose/Beeswax Edible Films Reinforced with Silver Nanoparticles. *Int. J. Biol. Macromol.* **2019**, *129*, 1103–1112. [[CrossRef](#)] [[PubMed](#)]
- Oyom, W.; Zhang, Z.; Bi, Y.; Tahergorabi, R. Application of Starch-Based Coatings Incorporated with Antimicrobial Agents for Preservation of Fruits and Vegetables: A Review. *Prog. Org. Coat.* **2022**, *166*, 106800. [[CrossRef](#)]
- Rojas-Graü, M.A.; Soliva-Fortuny, R.; Martín-Belloso, O. Edible Coatings to Incorporate Active Ingredients to Fresh-Cut Fruits: A Review. *Trends Food Sci. Technol.* **2009**, *20*, 438–447. [[CrossRef](#)]
- Dordevic Jancikova, S.; Dordević, D.; Sedlacek, P.; Kalina, M.; Těšíková, K.; Antonic, B.; Tremlová, B.; Treml, J.; Nejezchlebova, M.; Vapenka, L.; et al. Incorporation of Natural Blueberry, Red Grapes and Parsley Extract By-Products into the Production of Chitosan Edible Films. *Polymers* **2021**, *13*, 3388. [[CrossRef](#)] [[PubMed](#)]
- Tauferova, A.; Pospiech, M.; Javurkova, Z.; Tremlova, B.; Dordevic, D.; Jancikova, S.; Tesikova, K.; Zdarsky, M.; Vitez, T.; Vitezova, M. Plant Byproducts as Part of Edible Coatings: A Case Study with Parsley, Grape and Blueberry Pomace. *Polymers* **2021**, *13*, 2578. [[CrossRef](#)] [[PubMed](#)]
- Acevedo, C.A.; Lopez, D.A.; Tapia, M.J.; Enrione, J.; Skurtys, O.; Pedreschi, F.; Brown, D.I.; Creixell, W.; Osorio, F. Using RGB Image Processing for Designing an Alginate Edible Film. *Food Bioprocess Technol.* **2012**, *5*, 1511–1520. [[CrossRef](#)]

17. Sharma, G. *Color Fundamentals for Digital Imaging*, 1st ed.; CRC Press: Boca Raton, FL, USA, 2003; ISBN 9781315220086.
18. Luo, M.R. The CIE 2000 Colour Difference Formula: CIEDE2000. In Proceedings of the AIC: 9th Congress of the International Colour Association, Rochester, NY, USA, 24–29 June 2001; Volume 4421, pp. 554–559.
19. Navarro, R.; Arancibia, C.; Lidia Herrera, M.; Matiacevich, S. Effect of Type of Encapsulating Agent on Physical Properties of Edible Films Based on Alginate and Thyme Oil. *Food Bioprod. Processing* **2016**, *97*, 63–75. [[CrossRef](#)]
20. Li, J.; Sun, Q.; Sun, Y.; Chen, B.; Wu, X.; Le, T. Improvement of Banana Postharvest Quality Using a Novel Soybean Protein Isolate/Cinnamaldehyde/Zinc Oxide Bionanocomposite Coating Strategy. *Sci. Hortic.* **2019**, *258*, 108786. [[CrossRef](#)]
21. Saberli, B.; Thakur, R.; Vuong, Q.V.; Chockchaisawasdee, S.; Golding, J.B.; Scarlett, C.J.; Stathopoulos, C.E. Optimization of Physical and Optical Properties of Biodegradable Edible Films Based on Pea Starch and Guar Gum. *Ind. Crops Prod.* **2016**, *86*, 342–352. [[CrossRef](#)]
22. Wu, Y.; Zhang, W.; Yu, W.; Zhao, L.; Song, S.; Xu, W.; Zhang, C.; Ma, C.; Wang, L.; Wang, S. Study on the Volatile Composition of Table Grapes of Three Aroma Types. *LWT* **2019**, *115*, 108450. [[CrossRef](#)]
23. Zifkin, M.; Jin, A.; Ozga, J.A.; Zaharia, L.I.; Scherthner, J.P.; Gesell, A.; Abrams, S.R.; Kennedy, J.A.; Constabel, C.P. Gene Expression and Metabolite Profiling of Developing Highbush Blueberry Fruit Indicates Transcriptional Regulation of Flavonoid Metabolism and Activation of Abscisic Acid Metabolism. *Plant Physiol.* **2012**, *158*, 200–224. [[CrossRef](#)] [[PubMed](#)]
24. Marviziadeh, M.M.; Oladzadabbasabadi, N.; Mohammadi Nafchi, A.; Jokar, M. Preparation and Characterization of Bionanocomposite Film Based on Tapioca Starch/Bovine Gelatin/Nanorod Zinc Oxide. *Int. J. Biol. Macromol.* **2017**, *99*, 1–7. [[CrossRef](#)]
25. Mantilla, N.; Castell-Perez, M.E.; Gomes, C.; Moreira, R.G. Multilayered Antimicrobial Edible Coating and Its Effect on Quality and Shelf-Life of Fresh-Cut Pineapple (*Ananas Comosus*). *LWT Food Sci. Technol.* **2013**, *51*, 37–43. [[CrossRef](#)]
26. Zhao, Y.; McDaniel, M. 24—Sensory Quality of Foods Associated with Edible Film and Coating Systems and Shelf-Life Extension. In *Innovations in Food Packaging*; Han, J.H., Ed.; Food Science and Technology; Academic Press: London, UK, 2005; pp. 434–453. ISBN 978-0-12-311632-1.
27. Marchiore, N.G.; Manso, I.J.; Kaufmann, K.C.; Lemes, G.F.; de Oliveira Pizolli, A.P.; Droval, A.A.; Bracht, L.; Gonçalves, O.H.; Leimann, F.V. Migration Evaluation of Silver Nanoparticles from Antimicrobial Edible Coating to Sausages. *LWT Food Sci. Technol.* **2017**, *76*, 203–208. [[CrossRef](#)]
28. Rhim, J.W.; Wang, L.F.; Hong, S.I. Preparation and Characterization of Agar/Silver Nanoparticles Composite Films with Antimicrobial Activity. *Food Hydrocoll.* **2013**, *33*, 327–335. [[CrossRef](#)]
29. Dash, K.K.; Ali, N.A.; Das, D.; Mohanta, D. Thorough Evaluation of Sweet Potato Starch and Lemon-Waste Pectin Based-Edible Films with Nano-Titania Inclusions for Food Packaging Applications. *Int. J. Biol. Macromol.* **2019**, *139*, 449–458. [[CrossRef](#)]
30. Hou, X.; Xue, Z.; Liu, J.; Yan, M.; Xia, Y.; Ma, Z. Characterization and Property Investigation of Novel Eco-friendly Agar/Carrageenan/TiO<sub>2</sub> Nanocomposite Films. *J. Appl. Polym. Sci.* **2019**, *136*, 47113. [[CrossRef](#)]
31. Wardana, A.A.; Suyatma, N.E.; Muchtadi, T.R.; Yaliani, S. Influence of ZnO Nanoparticles and Stearic Acid on Physical, Mechanical and Structural Properties of Cassava Starch-Based Bionanocomposite Edible Films. *Int. Food Res. J.* **2018**, *25*, 1837–1844.
32. Bakhy, E.A.; Zidan, N.S.; Aboul-Anean, H.E.D. The Effect of Nano Materials On Edible Coating and Films' Improvement. *Int. J. Pharm. Res. Allied Sci.* **2018**, *7*, 20–41.
33. Kumar, S.; Shukla, A.; Baul, P.P.; Mitra, A.; Halder, D. Biodegradable Hybrid Nanocomposites of Chitosan/Gelatin and Silver Nanoparticles for Active Food Packaging Applications. *Food Packag. Shelf Life* **2018**, *16*, 178–184. [[CrossRef](#)]
34. Feng, Z.; Li, L.; Wang, Q.; Wu, G.; Liu, C.; Jiang, B.; Xu, J. Effect of Antioxidant and Antimicrobial Coating Based on Whey Protein Nanofibrils with TiO<sub>2</sub> Nanotubes on the Quality and Shelf Life of Chilled Meat. *Int. J. Mol. Sci.* **2019**, *20*, 1184. [[CrossRef](#)] [[PubMed](#)]
35. Li, Y.; Jiang, Y.; Liu, F.; Ren, F.; Zhao, G.; Leng, X. Fabrication and Characterization of TiO<sub>2</sub>/Whey Protein Isolate Nanocomposite Film. *Food Hydrocoll.* **2011**, *25*, 1098–1104. [[CrossRef](#)]
36. Gohargani, M.; Lashkari, H.; Shirazinejad, A. Study on Biodegradable Chitosan-Whey Protein-Based Film Containing Bionanocomposite TiO<sub>2</sub> and Zataria Multiflora Essential Oil. *J. Food Qual.* **2020**, *2020*, 8844167. [[CrossRef](#)]
37. Le, K.H.; Dac-Binh Nguyen, M.; Dai Tran, L.; Phuong, H.; Thi, N.; Van Tran, C.; Van Tran, K.; Phuong, H.; Thi, N.D.; Yoon, Y.S.; et al. A Novel Antimicrobial ZnO Nanoparticles-Added Polysaccharide Edible Coating for the Preservation of Postharvest Avocado under Ambient Conditions. *Prog. Org. Coat.* **2021**, *158*, 106339. [[CrossRef](#)]